IEEE Access
Multidisciplinary ⋮ Rapid Review ⋮ Open Access Journal

Received 10 January 2023, accepted 23 January 2023, date of publication 30 January 2023, date of current version 8 February 2023.

Digital Object Identifier 10.1109/ACCESS.2023.3240742

RESEARCH ARTICLE

Equivalence Analysis of Cascade Control for a Class of Cascade Integral Systems

PING LIN[1,2], YAN SHI[1,2], AND XUE-FANG WANG[1,2,3], (Member, IEEE)

[1]Key Laboratory of Intelligent Control and Optimization for Industrial Equipment of Ministry of Education, Dalian University of Technology, Dalian 116024, China
[2]School of Control Science and Engineering, Dalian University of Technology, Dalian 116024, China
[3]Aeronautical and Automotive Engineering, Loughborough University, LE11 3TU Loughborough, U.K.

Corresponding author: Ping Lin (dmulinping@dlut.edu.cn)

This work was supported by the National Natural Science Foundation of China under Grant 62203085 and Grant 62103078.

ABSTRACT A class of generalized proportional-integral-derivative (PID) control with feedforward compensation (FFC) is obtained for a class of cascade integral systems by equivalence analysis of the cascade control and such the analysis is obtained by using the information of the model and outermost loop feedback. Firstly, a new type of error related to the traditional error such as proportional (P) or proportional integral (PI) is given. Secondly, by analyzing cascade control for a class of ideal cascade integral systems, the generalized PID control with FFC is presented based on the proposed new type of error. Then, the generalized PID control with FFC is extended to a class of non-ideal cascade integral systems to reduce the number of feedback loop and sensors. Finally, the simulation results of the speed/position servo system of direct current motor are given to verify the theoretical analysis results.

INDEX TERMS Equivalence analysis of cascade control, generalized PID control, class of cascade integral systems, new definition of the traditional error.

I. INTRODUCTION

Electrical machine drive system used to develop electrification has been widely applied to aerospace, aviation, navigation, land transportation and other scenarios. Especially, developing high reliable and efficient electrification technology is of critical importance for the aviation industry due to the following advantages. Firstly, it can sharply decrease the workload of maintenance and enhance the flexibility of operability [1]. Secondly, it can significantly reduce man-made CO_2 emissions [2], which will make civil aircraft more environmentally friendly. Furthermore, the revolutionary of full electrification eliminates mechanical, hydraulic and pneumatic power systems for auxiliary power unit or starter/generator in aircraft, which can lighten the weight of aircraft and then reduces the specific fuel consumption of aircraft engine [1]. Furthermore, electrical machines are the significant part of the more electric aircraft [1].

The associate editor coordinating the review of this manuscript and approving it for publication was Qi Zhou.

Control structure is one of the most significant parts for electrical machine drive system, which affect the operation performance. The most common used control structure of electrical machine drive system is two-stage or three-stage cascade control structures (see [3], [4], [5]). To be specific, the starter/generator of gas turbine engine always adopts two-stage proportional-integral (PI) cascade control to realize the speed tracking control or torque tracking control in starter mode and set-point voltage control in generator mode [6]. The same cascade control structure is also applied in electric fuel pumps scenarios. Furthermore, electro-hydrostatic actuators (EHA) and electro-mechanical actuators (EMA) adopt three-stage proportional-integral cascade control in more electric aircraft (MEA) and more electric engine (MEE) [7]. Besides, electric flap surface actuator, one of the most significant pieces of equipment on the aircraft, adopts three-stage PI cascade control to achieve a desired control effect [8], [9].

In addition, cascade control structures are introduced in [10], [11], [12], [13], and [14]. Cascade control structure is realized by sensors feedback. For example, the three-stage

cascade control of electrical machines includes the outermost loop sensor named position loop, the middle loop named speed loop and the inner loop named current loop. The corresponding feedback is realized by position sensors, speed sensors and current sensors, respectively. However, not all states are measurable in the engineering scenarios, such as the solar panel of space station. Therefore, in such cases, the state feedback method may not be applied, which may be replaced by observers based on output feedback (see [15]). Or some other elaborated robust algorithms are thoroughly studied in [16], [17], [18], [19], and [20] to address the similar problems.

In the cascade control structures, while many sensors used for feedback control may increase hardware costs of control system and the probability of equipment failure (see [21], [22]). In addition, the existence of uncertainties or delays in the sensors is inevitable [23], [24]. Decreasing the number of sensors in cascade control is encouraged to be investigated. Thus, it is necessary to propose a new control structure to reduce the dependence on sensors feedback without sacrificing control performance. In the other hand, some models have also been transformed into a cascade form such that some analysis methods can be applied, i.e., the "analytic" cascade system. For example, the reference transforms linear systems into a cascade form to address the mismatching disturbances [25]. In [26], the method is used to analyze the existence of solution to the distributed optimal coordination.

Motivated by the above observations, this paper proposes a class of new control structures relative to the generalized PID control by making the equivalent analysis of cascade control based on model information.

The main contributions of this paper can be summarized as follows. Firstly, for any cascade integral system, we propose a new generalized PID control structure with FFC based on generalized error, which can be used to make the equivalence analysis for different kinds of cascade control structures. This point is proved mathematically in this paper. Secondly, compared with the traditional methods [10], [11], [12], [13], [14], the proposed method uses only the outermost loop feedback which can reduce the number of feedback loops and sensors and without sacrificing control performance. In addition, direct current motor speed/position systems are given to verify the theoretical analysis and also show that the control performance of the generalized PID control with FFC is satisfactory.

The rest of this paper is organized as follows. Section 2 formulates the problem. The generalized PID control with FFC derived from cascade control structures is presented for ideal cascade integral systems in Section 3. Section 4 gives the generalized PID control with FFC for non-ideal cascade integral systems. Section 5 gives simulation results and discussions. Conclusions and future work appear in Section 6.

II. PROBLEM FORMULATIONS

The current and speed cascade system of a direct current (DC) motor shown in (1) and the current, speed and position cascade system of a DC motor presented in (2) are prevalent.

$$\begin{cases} \dot{\omega}_m = \dfrac{-B_m\omega_m - T_L}{J_m} + \dfrac{K_t i_a}{J_m}, \\ \dot{i}_a = -\dfrac{R_a i_a + K_b\omega_m}{L_a} + \dfrac{\upsilon_a}{L_a}, \end{cases} \tag{1}$$

$$\begin{cases} \dot{\theta} = \omega_m, \\ \dot{\omega}_m = \dfrac{-B_m\omega_m - T_L}{J_m} + \dfrac{K_t i_a}{J_m}, \\ \dot{i}_a = -\dfrac{R_a i_a + K_b\omega_m}{L_a} + \dfrac{\upsilon_a}{L_a}, \end{cases} \tag{2}$$

where i_a is the armature current, θ is the angle of the DC motor rotor, R_a is the armature resistance, L_a is the armature inductance, ω_m is the rotor angle speed, K_b is the back electromotive force coefficient, υ_a is the input voltage, J_m is the rotor inertia, B_m is the friction coefficient, T_L is the load torque disturbances and K_t is the torque constant.

The traditional error is defined as the error between the reference value and the feedback value, i.e., $e_0 = x_{11}^{ref} - x_{11}$, where x_{11}^{ref} and x_{11} are given in Figure 1. In this paper, we employ the definition of generalized error in control systems, namely P, integral (I), proportional-derivative (PD), PID or other types of the traditional error, to obtain the corresponding generalized PID control.

Note that (1) illustrates that the outermost loop controlled variable is the speed. (2) shows that the outermost loop controlled variable is the position. The three-stage and two-stage cascade PI control structures are prevalently adopted to regulate the position and the speed in electrical machine systems, respectively. By analyzing the cascade control, we aim to reveal the relationship between the cascade control and its corresponding generalized PID control. Firstly, we analyze the ideal cascade integral systems. Then the corresponding results are extended to the non-ideal cascade integral systems. Furthermore, the generalized PID control will be presented as the $\mathrm{PI}^{m_1}\mathrm{I}^{m_2}\mathrm{D}^{n_1}\mathrm{D}^{n_2}$ control, where $n_i \in N$, $m_i \in N$ and $i \in \{1, 2\}$. N is a set of nonnegative integers. $\dot{k}$ stands for $\frac{dk}{dt}$.

III. GENERALIZED PID CONTROL FOR IDEAL CASCADE INTEGRAL SYSTEMS

In this section, for a class of cascade integral systems, the analysis of cascade control structures, namely PI control, P control and hybrid control of PI and P, is presented in details.

(1) and (2) can be recast as

$$\begin{cases} \dot{\omega}_m = f_1 + \dfrac{K_t i_a}{J_m}, \\ \dot{i}_a = f_2 + \dfrac{\upsilon_a}{L_a}, \end{cases} \tag{3}$$

$$\begin{cases} \dot{\theta} = \omega_m, \\ \dot{\omega}_m = f_1 + \dfrac{K_t i_a}{J_m}, \\ \dot{i}_a = f_2 + \dfrac{\upsilon_a}{L_a}, \end{cases} \tag{4}$$

where $f_1 = \frac{-B_m\omega_m - T_L}{J_m}$ and $f_2 = -\frac{R_a i_a + K_b\omega_m}{L_a}$. In order to simplify the analysis of cascade control, when $f_1 = 0$ and $f_2 = 0$, (3) can be generalized to be described by (5), (6). (4) can be generalized to be described by (7), (8) and (9). Thus, an ideal second-order cascade system and an ideal third-order cascade system, illustrated in Figure 1 and Figure 2, are ideal cascade integral systems.

The prerequisite is that x_{11}^{ref} is constant reference value. x_{11}, x_{21} and x_{31} are the feedback values which can be measured. u_1 is control input. Y is a measurable output vector. a_{121}, a_{122}, b_2, b_3 are positive constants. kp_{11}, kp_{21}, kp_{31}, ki_{11}, ki_{21} and ki_{31} are gain coefficients of controllers.

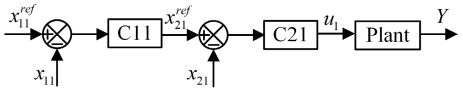

FIGURE 1. The diagram of two-stage cascade control.

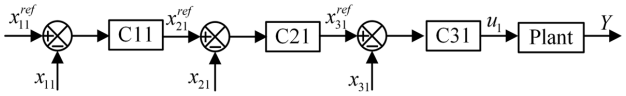

FIGURE 2. The diagram of three-stage cascade control.

To be more specific, the plant in the second-order cascade integral system of the closed-loop in Figure 1 can be given as follows:

$$\dot{x}_{11} = a_{121}x_{21}, \tag{5}$$
$$\dot{x}_{21} = b_2u_1. \tag{6}$$

The plant in the third-order cascade integral system of the closed-loop in Figure 2 can be described as follows:

$$\dot{x}_{11} = a_{121}x_{21}, \tag{7}$$
$$\dot{x}_{21} = a_{122}x_{31}, \tag{8}$$
$$\dot{x}_{31} = b_3u_1. \tag{9}$$

A. EQUIVALENCE ANALYSIS OF PI CASCADE CONTROL

In this subsection, one lemma is presented to show such generalized PID control.

Lemma 1: For the systems which can be changed into the ideal cascade integral systems, the corresponding cascade control structures based on PI control can be interpreted as a class of the generalized PID control with FFC based on the generalized error.

Proof: In this subsection, two-stage cascade control system will be first presented. The C11 and C21 in Figure 1 can be shown as follows:

$$x_{21}^{ref} = kp_{11}(x_{11}^{ref} - x_{11}) + ki_{11}\int(x_{11}^{ref} - x_{11})dt, \tag{10}$$
$$u_1 = kp_{21}(x_{21}^{ref} - x_{21}) + ki_{21}\int(x_{21}^{ref} - x_{21})dt. \tag{11}$$

The equations (10) and (11) can be illustrated in Figure 3.

Substituting (5) and (10) into (11), we obtain

$$\begin{aligned} u_1 = {} & kp_{21}kp_{11}(x_{11}^{ref} - x_{11}) + ki_{21}kp_{11}\int(x_{11}^{ref} - x_{11})dt \\ & + ki_{11}kp_{21}\int(x_{11}^{ref} - x_{11})dt - \frac{ki_{21}}{a_{121}}\int\dot{x}_{11}dt \\ & + ki_{11}ki_{21}\int\Big(\int(x_{11}^{ref} - x_{11})dt\Big)dt - \frac{kp_{21}}{a_{121}}\dot{x}_{11}. \end{aligned} \tag{12}$$

Remark 1: The generalized error can be defined as the PI of the traditional error, which are shown in equations (13), (18) and (39). Because x_1^{ref} is constant, then (12) can be recast as

$$\begin{aligned} u_1 = {} & kp_{21}kp_{11}(x_{11}^{ref} - x_{11}) + ki_{21}kp_{11}\int(x_{11}^{ref} - x_{11})dt \\ & + ki_{11}kp_{21}\int(x_{11}^{ref} - x_{11})dt \\ & + \frac{ki_{21}}{a_{121}}\int(\dot{x}_{11}^{ref} - \dot{x}_{11})dt - \frac{ki_{21}}{a_{121}}\int(\dot{x}_{11}^{ref})dt \\ & + ki_{11}ki_{21}\int\Big(\int(x_{11}^{ref} - x_{11})dt\Big)dt + \frac{kp_{21}}{a_{121}}(\dot{x}_{11}^{ref} - \dot{x}_{11}). \end{aligned}$$

Define the generalized error

$$e_1 = kp_{21}(x_{11}^{ref} - x_{11}) + ki_{21}\int(x_{11}^{ref} - x_{11})dt, \tag{13}$$

then we have

$$u_1 = kp_{11}e_1 + ki_{11}\int e_1dt + \frac{\dot{e}_1}{a_{121}} - \frac{ki_{21}}{a_{121}}x_{11}^{ref}, \tag{14}$$

The equation (14) can be shown in Figure 4, which reveals that (14) can be interpreted as a generalized PID controller with FFC.

Next, we show the analysis of three-stage cascade control system. In Figure 2, C11, C21 and C31 adopt PI controllers yielding

$$x_{21}^{ref} = kp_{11}(x_{11}^{ref} - x_{11}) + ki_{11}\int(x_{11}^{ref} - x_{11})dt, \tag{15}$$
$$x_{31}^{ref} = kp_{21}(x_{21}^{ref} - x_{21}) + ki_{21}\int(x_{21}^{ref} - x_{21})dt, \tag{16}$$
$$u_1 = kp_{31}(x_{31}^{ref} - x_{31}) + ki_{31}\int(x_{31}^{ref} - x_{31})dt. \tag{17}$$

The equations (15), (16) and (17) can be described as in Figure 5. Substituting (7), (8), (15) and (16) into (17), we have $u_1 = P_1 + P_2 + P_3$, where

$$\begin{aligned} P_1 = {} & kp_{11}kp_{21}kp_{31}(x_{11}^{ref} - x_{11}) + \frac{ki_{21}}{a_{121}}kp_{31}\int(\dot{x}_{11}^{ref} - \dot{x}_{11})dt \\ & + ki_{11}kp_{21}kp_{31}\int(x_{11}^{ref} - x_{11})dt \\ & + kp_{11}ki_{21}kp_{31}\int(x_{11}^{ref} - x_{11})dt, \\ P_2 = {} & (ki_{11}ki_{21}kp_{31})\int\Big(\int(x_{11}^{ref} - x_{11})dt\Big)dt \\ & + \frac{kp_{21}}{a_{121}}kp_{31}(\dot{x}_{11}^{ref} - \dot{x}_{11}) + kp_{31}\frac{\ddot{x}_{11}^{ref} - \ddot{x}_{11}}{a_{121}a_{122}} \\ & + (kp_{11}kp_{21}ki_{31})\int(x_{11}^{ref} - x_{11})dt \end{aligned}$$

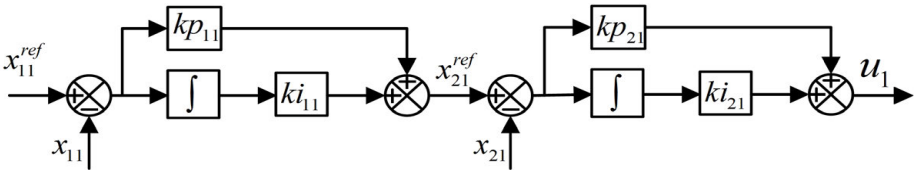

FIGURE 3. Detailed structure of the PI-PI cascade control.

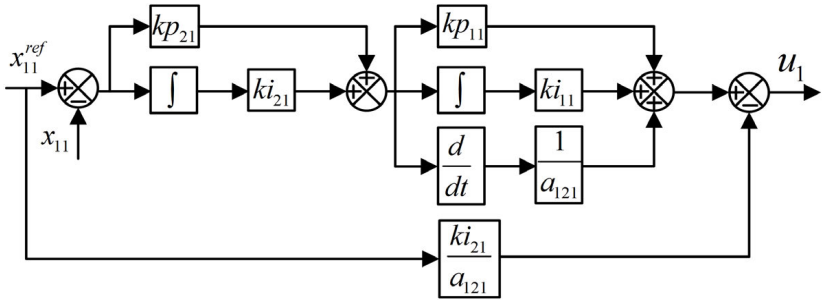

FIGURE 4. Equivalence control structure of the PI-PI cascade control.

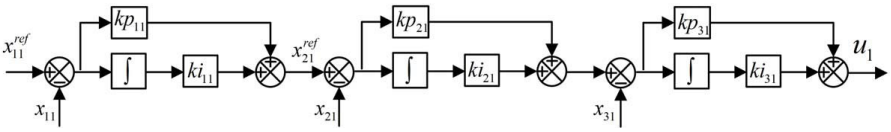

FIGURE 5. Detailed structure of the PI-PI-PI cascade control.

$$+\frac{ki_{21}}{a_{121}}ki_{31}\int\Big(\int(\dot{x}_{11}^{ref}-\dot{x}_{11})dt\Big)dt$$
$$+(ki_{11}kp_{21}ki_{31})\int\Big(\int(x_{11}^{ref}-x_{11})dt\Big)dt,$$
$$P_3=(kp_{11}ki_{21}ki_{31})\int\Big(\int(x_{11}^{ref}-x_{11})dt\Big)dt$$
$$+ki_{11}ki_{21}ki_{31}\int\Big(\int\Big(\int(x_{11}^{ref}-x_{11})dt\Big)dt\Big)dt$$
$$+\frac{kp_{21}}{a_{121}}ki_{31}\int(\dot{x}_{11}^{ref}-\dot{x}_{11})dt+ki_{31}\int(\frac{\ddot{x}_{11}^{ref}-\ddot{x}_{11}}{a_{121}a_{122}})dt$$
$$-ki_{21}ki_{31}\frac{\int x_{11}^{ref}dt}{a_{121}}-(kp_{21}ki_{31}+kp_{31}ki_{21})\frac{x_{11}^{ref}}{a_{121}}.$$

Define the generalized error

$$e_{21}=kp_{31}(x_{11}^{ref}-x_{11})+ki_{31}\int(x_{11}^{ref}-x_{11})dt. \quad (18)$$

Then u_1 is rewritten as

$$u_1=(kp_{11}kp_{21}+\frac{ki_{21}}{a_{121}})e_{21}+ki_{21}ki_{11}\int\Big(\int e_{21}dt\Big)dt$$
$$+(ki_{11}kp_{21}+kp_{11}ki_{21})\int e_{21}dt-ki_{21}ki_{31}\frac{\int x_{11}^{ref}dt}{a_{121}}$$
$$+\frac{kp_{21}}{a_{121}}\dot{e}_{21}+\frac{1}{a_{121}a_{122}}\ddot{e}_{21}-(kp_{21}ki_{31}+kp_{31}ki_{21})\frac{x_{11}^{ref}}{a_{121}}. \quad (19)$$

The (19) can be seen as a generalized PII^{2}DD^2 controller with FFC, which can be illustrated in Figure 6. The proof of Lemma 1 is finished. ■

B. EQUIVALENCE ANALYSIS OF P CASCADE CONTROL

In this subsection, we use one lemma to show the analysis of P cascade control.

Lemma 2: For the systems which can be changed into the ideal cascade integral systems, the corresponding cascade control structures based on P control can be interpreted as a class of the generalized PID control based on the generalized error.

Proof: We first consider two-stage cascade control system. In Figure 1, both C11 and C21 use P control, which can be described as follows:

$$x_{21}^{ref}=kp_{11}(x_{11}^{ref}-x_{11}), \quad (20)$$
$$u_1=kp_{21}(x_{21}^{ref}-x_{21}). \quad (21)$$

The equations (20) and (21) are shown in Figure 7. Substituting (5) and (20) into (21), we can obtain

$$u_1=kp_{21}kp_{11}(x_{11}^{ref}-x_{11})-kp_{21}\frac{\dot{x}_{11}}{a_{121}}. \quad (22)$$

Remark 2: The generalized error can be defined as the P of the traditional error, which are illustrated in the equations (23), (29) and (34).

Define the generalized error

$$e_3=kp_{21}(x_{11}^{ref}-x_{11}). \quad (23)$$

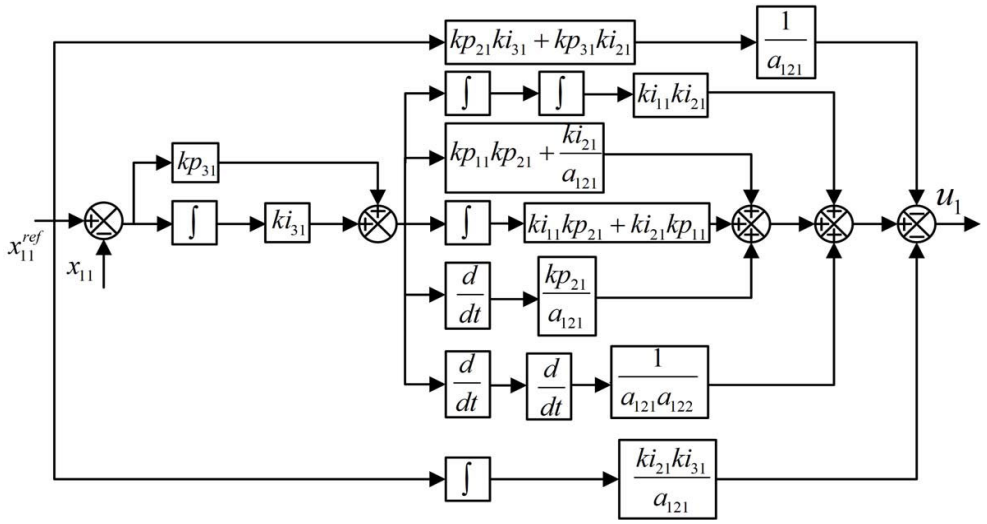

FIGURE 6. Equivalence control structure of the PI-PI-PI cascade control.

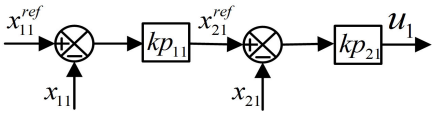

FIGURE 7. Detailed structure of the P-P cascade control.

Then (22) can be rewritten as

$$u_1 = kp_{11}e_3 + \frac{\dot{e}_3}{a_{121}}. \tag{24}$$

Therefore, (24) shown in Figure 8 can be seen as a PD controller. Next, three-stage cascade control system is analyzed. All C11, C21 and C31 employ P control, which can be written as follows:

$$x_{21}^{ref} = kp_{11}(x_{11}^{ref} - x_{11}), \tag{25}$$

$$x_{31}^{ref} = kp_{21}(x_{21}^{ref} - x_{21}), \tag{26}$$

$$u_1 = kp_{31}(x_{31}^{ref} - x_{31}). \tag{27}$$

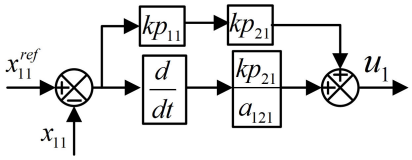

FIGURE 8. Equivalence control structure of the P-P cascade control.

The equations (25), (26) and (27) are shown in Figure 9. Substituting (7), (8), (25) and (26) into (27), we obtain

$$u_1 = kp_{31}kp_{21}kp_{11}(x_{11}^{ref} - x_{11}) - kp_{31}kp_{21}\frac{\dot{x}_{11}}{a_{121}} - kp_{31}\frac{\ddot{x}_{11}}{a_{121}a_{122}}. \tag{28}$$

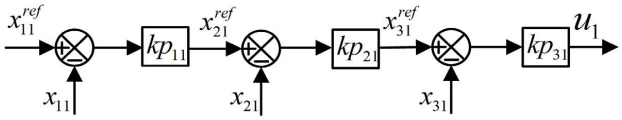

FIGURE 9. Detailed structure of the P-P-P cascade control.

Remark 3: The generalized error can be defined as the P of the traditional error. Define the generalized error

$$e_4 = kp_{31}(x_{11}^{ref} - x_{11}). \tag{29}$$

Thus, (28) can be rewritten as

$$u_1 = kp_{21}kp_{11}e_4 + kp_{21}\frac{\dot{e}_4}{a_{121}} + \frac{\ddot{e}_4}{a_{121}a_{122}}. \tag{30}$$

So (30) can be regarded as a generalized proportional derivative derivative-derivative (PDD^2) controller, which is shown in Figure 10. The proof of Lemma 2 is finished. ■

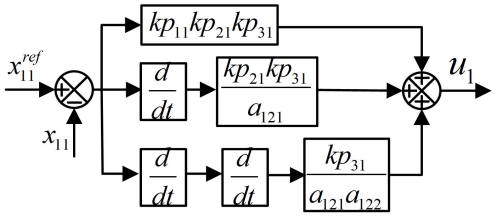

FIGURE 10. Equivalence control structure of the P-P-P cascade control.

C. EQUIVALENCE ANALYSIS OF HYBRID CASCADE CONTROL

In some industrial scenarios, the outer loop adopts PI control structure and the inner loop uses P control structure so as to increase the response speed of the manipulated variables. We use the following lemma to show this point.

Lemma 3: For the systems which can be changed into the ideal cascade integral systems, the corresponding cascade control structures based on hybrid control of P and PI can be interpreted as a class of the generalized PID control with FFC based on the generalized error.

Proof: We first consider two-stage cascade control system. C11 and C21 in Figure 1 are designed as PI and P controllers, respectively, which are shown in Figure 11.

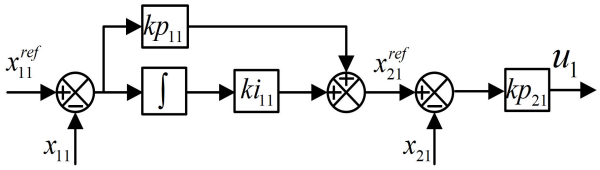

FIGURE 11. Detailed structure of the PI-P cascade control.

The mathematical expressions can be described as follows:

$$x_{21}^{ref} = kp_{11}(x_{11}^{ref} - x_{11}) + ki_{11}\int (x_{11}^{ref} - x_{11})dt, \quad (31)$$

$$u_1 = kp_{21}(x_{21}^{ref} - x_{21}). \quad (32)$$

Substituting (5) and (31) into (32) yields

$$u_1 = kp_{21}kp_{11}(x_{11}^{ref} - x_{11}) - kp_{21}\frac{\dot{x}_{11}}{a_{121}} + kp_{21}ki_{11}\int (x_{11}^{ref} - x_{11})dt. \quad (33)$$

Remark 4: The generalized error can be defined as the P of the traditional error. Denote the generalized error

$$e_5 = kp_{21}(x_{11}^{ref} - x_{11}). \quad (34)$$

Then (33) can be rewritten as

$$u_1 = kp_{11}e_5 + ki_{11}\int e_5 dt + \frac{\dot{e}_5}{a_{121}}. \quad (35)$$

Thus, (35) can be regarded as a generalized PID controller, which is illustrated in Figure 12.

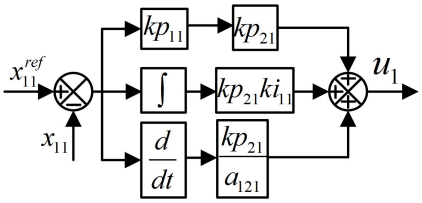

FIGURE 12. Equivalence control structure of the PI-P cascade control.

Now we consider three-stage cascade control system. Controllers C11, C21 and C31 in Figure 2 employ P, PI and PI, respectively, which can be illustrated as follows:

$$x_{21}^{ref} = kp_{11}(x_{11}^{ref} - x_{11}), \quad (36)$$

$$x_{31}^{ref} = kp_{21}(x_{21}^{ref} - x_{21}) + ki_{21}\int (x_{21}^{ref} - x_{21})dt, \quad (37)$$

$$u_1 = kp_{31}(x_{31}^{ref} - x_{31}) + ki_{31}\int (x_{31}^{ref} - x_{31})dt. \quad (38)$$

The equations (36), (37) and (38) are shown in Figure 13. Substitute (7), (8), (36) and (37) into (38).

Remark 5: The generalized error can be defined as the PI of the traditional error. and define the generalized error

$$e_6 = kp_{31}(x_{11}^{ref} - x_{11}) + ki_{31}\int (x_{11}^{ref} - x_{11})dt, \quad (39)$$

Then we obtain

$$u_1 = (kp_{21}kp_{11} + \frac{ki_{21}}{a_{121}})e_6 + ki_{21}kp_{11}\int e_6 dt + kp_{21}\frac{\dot{e}_6}{a_{121}} + \frac{\ddot{e}_6}{a_{121}a_{122}} - ki_{21}ki_{31}\frac{\int x_{11}^{ref}dt}{a_{121}} - (kp_{21}ki_{31} + kp_{31}ki_{21})\frac{x_{11}^{ref}}{a_{121}}. \quad (40)$$

So (40) can be treated as a generalized PIDD^2 controller with FFC, which is illustrated in Figure 14. The proof of Lemma 3 is finished. ■

D. A GENERALIZED PID CONTROL

In subsections A, B, C derivation process is another way to analyze cascade control for the second-order and third-order cascade integral systems. To show the analysis of cascade control, we present the following theorem based on the conclusions of Lemma 1, Lemma 2 and Lemma 3.

Theorem 1: For the systems which can be changed into the cascade integral systems, the corresponding cascade control structures based on P control, PI control or hybrid control of P and PI can be interpreted as a class of the generalized PID control with FFC based on the generalized error.

Proof: The conclusion of Theorem 1 can be easily proved by referring to Lemmas 1, 2 and 3. To be more specific, Lemma 1 illustrates that the cascade control based on PI control can be interpreted as a class of the generalized PID control with FFC; Lemma 2 presents that the cascade control based on P control is regarded as a class of the generalized PID control; Lemma 3 shows that the cascade control based on hybrid control of P and PI can be interpreted as a class of the generalized PID control with FFC. So the proof of Theorem 1 is finished. ■

IV. GENERALIZED PID CONTROL FOR NON-IDEAL CASCADE INTEGRAL SYSTEMS

Section III illustrates the generalized PID control for ideal cascade integral systems. However, it is prevalent that the controlled plants are non-ideal cascade integral systems. Thus, it is meaningful to extend the results of Section III to non-ideal cascade integral systems. Thus, we propose the generalized PID control with FFC for speed/position servo systems of direct current motor, which is originated from the cascade control.

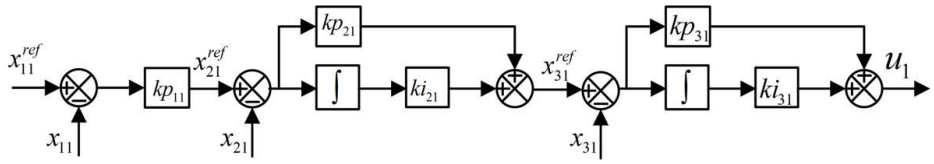

FIGURE 13. Detailed structure of the P-PI-PI cascade control.

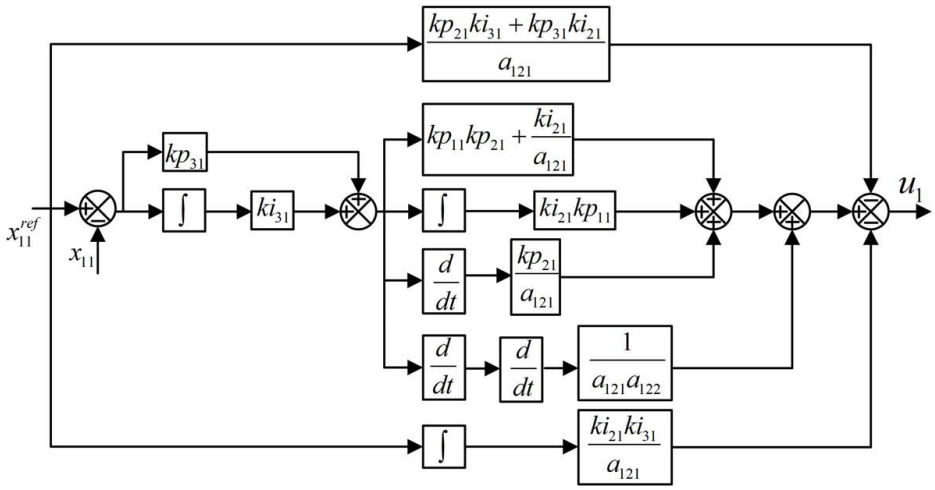

FIGURE 14. Equivalence control structure of the P-PI-PI cascade control.

A. A GENERALIZED PID CONTROL FOR SPEED SERVO SYSTEM

Lemma 4: For the systems (1), the corresponding cascade control structures based on PI control with FFC can be interpreted as a class of the generalized PID control with FFC.

Proof: As for (1), there exists a PI-PI cascade structure, which can be illustrated as follows:

$$\upsilon_a = \omega_c L_a(i_a^* - i_a) + \omega_c R_a \int (i_a^* - i_a)dt + K_b\omega_m, \quad (41)$$

$$i_a^* = \frac{\omega_s J_m}{K_t}(\omega_m^* - \omega_m) + \frac{\omega_s B_m}{K_t}\int (\omega_m^* - \omega_m)dt + \frac{T_L}{K_t}, \quad (42)$$

where ω_m^* and i_a^* are reference values.

Substituting (42) into (41), we can obtain

$$\begin{aligned}\upsilon_a = {} & \omega_c L_a[(\frac{\omega_s J_m}{K_t}(\omega_m^* - \omega_m) \\ & + \frac{\omega_s B_m}{K_t}\int (\omega_m^* - \omega_m)dt + \frac{T_L}{K_t}) - i_a] \\ & + \omega_c R_a \int [\frac{\omega_s J_m}{K_t}(\omega_m^* - \omega_m)]dt \\ & + \omega_c R_a \int [\frac{\omega_s B_m}{K_t}\int (\omega_m^* - \omega_m)dt + \frac{T_L}{K_t} - i_a]dt + K_b\omega_m. \end{aligned} \quad (43)$$

According to $i_a = \frac{J_m\dot{\omega}_m}{K_t} + \frac{\omega_m B_m}{K_t} + \frac{T_L}{K_t}$, (43) can be recast as

$$\begin{aligned}\upsilon_a = {} & \omega_c L_a[\frac{\omega_s J_m + B_m}{K_t}(\omega_m^* - \omega_m) + \frac{\omega_s B_m}{K_t}\int (\omega_m^* - \omega_m)dt \\ & + \frac{J_m}{K_t}(\dot{\omega}_m^* - \dot{\omega}_m) - \frac{J_m\dot{\omega}_m^*}{K_t} - \frac{\omega_m^* B_m}{K_t}] \\ & + \omega_c R_a \int [\frac{\omega_s J_m + B_m}{K_t}(\omega_m^* - \omega_m)]dt \\ & + \omega_c R_a \int [\frac{\omega_s B_m}{K_t}\int (\omega_m^* - \omega_m)dt]dt \\ & + \omega_c R_a \int [\frac{J_m}{K_t}(\dot{\omega}_m^* - \dot{\omega}_m)]dt \\ & + \omega_c R_a \int [-\frac{J_m\dot{\omega}_m^*}{K_t} - \frac{\omega_m^* B_m}{K_t}]dt + K_b\omega_m. \end{aligned} \quad (44)$$

Defining the error $e_7 = \omega_c(\omega_m^* - \omega_m)$, (44) can be rewritten as

$$\begin{aligned}\upsilon_a = {} & L_a[\frac{\omega_s J_m + B_m}{K_t}e_7 + \frac{\omega_s B_m}{\omega_c K_t}\int e_7 dt + \frac{J_m}{\omega_c K_t}(\dot{e}_7)] \\ & - \frac{J_m\dot{\omega}_m^*}{K_t}\omega_c L_a - \frac{\omega_m^* B_m}{K_t}\omega_c L_a \\ & + R_a \int [\frac{\omega_s J_m + B_m}{K_t}e_7 + \frac{\omega_s B_m}{\omega_c K_t}\int e_7 dt + \frac{J_m}{\omega_c K_t}(\dot{e}_7)]dt \\ & - \omega_c R_a \int [\frac{\omega_m^* B_m}{K_t}]dt - \omega_c R_a \frac{J_m\omega_m^*}{K_t} + K_b\omega_m. \end{aligned} \quad (45)$$

In (45), the mathematical terms $-\frac{J_m\dot{\omega}_m^*}{K_t}\omega_c L_a - \frac{\omega_m^* B_m}{K_t}\omega_c L_a$ and $-\omega_c R_a \int [\frac{\omega_m^* B_m}{K_t}]dt - \omega_c R_a \frac{J_m\omega_m^*}{K_t} + K_b\omega_m$ can be regarded as FFC. Thus, (45) can be seen as a PII^{2}D control with FFC. The proof of Lemma 4 is finished. ■

B. A GENERALIZED PID CONTROL FOR POSITION SERVO SYSTEM

Lemma 5: For the systems (2), the corresponding cascade control structures based on hybrid control of P and PI control with FFC can be interpreted as a class of the generalized PID control with FFC.

Proof: For (2), it is prevalent that the position loop adopts P controller, and the speed loop and current loop both use PI controllers. That is to say, $\omega_m^*=k_p(\theta_m^*-\theta_m)$, where θ_m^* is a reference value. Then we have

$$\begin{aligned}\upsilon_a &= \omega_c L_a[\frac{\omega_s J_m}{K_t}[k_p(\theta_m^*-\theta_m)-\omega_m]\\ &+\frac{\omega_s B_m}{K_t}\int[k_p(\theta_m^*-\theta_m)-\omega_m]dt\\ &-\frac{J_m\dot{\omega}_m}{K_t}-\frac{\omega_m B_m}{K_t}]\\ &+\omega_c R_a\int[\frac{\omega_s J_m}{K_t}[k_p(\theta_m^*-\theta_m)-\omega_m]]dt\\ &+\omega_c R_a\int[\frac{\omega_s B_m}{K_t}\int[k_p(\theta_m^*-\theta_m)-\omega_m]dt]dt\\ &+\omega_c R_a\int[-\frac{J_m\dot{\omega}_m}{K_t}-\frac{\omega_m B_m}{K_t}]dt+K_b\omega_m. \end{aligned}\tag{46}$$

From $\dot{\theta}_m=\omega_m$, (46) can be recast as

$$\begin{aligned}\upsilon_a &= \omega_c L_a\frac{\omega_s J_m}{K_t}k_p(\theta_m^*-\theta_m)-\omega_c L_a\frac{\omega_s J_m}{K_t}\dot{\theta}_m\\ &+\omega_c L_a\frac{\omega_s B_m}{K_t}k_p\int(\theta_m^*-\theta_m)dt-\omega_c L_a\frac{\omega_s B_m}{K_t}\int\dot{\theta}_m dt\\ &-\omega_c L_a\frac{J_m\ddot{\theta}_m}{K_t}-\omega_c L_a\frac{\dot{\theta}_m B_m}{K_t}\\ &+\omega_c R_a\frac{\omega_s J_m}{K_t}k_p\int(\theta_m^*-\theta_m)dt-\omega_c R_a\frac{\omega_s J_m}{K_t}\int\dot{\theta}_m dt\\ &+\omega_c R_a\frac{\omega_s B_m}{K_t}k_p\int\int(\theta_m^*-\theta_m)dtdt\\ &-\omega_c R_a\frac{\omega_s B_m}{K_t}\int\int\dot{\theta}_m dtdt\\ &-\omega_c R_a\int[\frac{J_m\ddot{\theta}_m}{K_t}+\frac{\dot{\theta}_m B_m}{K_t}]dt\\ &+K_b\dot{\theta}_m. \end{aligned}\tag{47}$$

Defining $e_8=k_p(\theta_m^*-\theta_m)$, (47) can be rewritten as

$$\begin{aligned}\upsilon_a &= \omega_c L_a\frac{\omega_s J_m}{K_t}e_8-\omega_c L_a\frac{\omega_s J_m}{K_t}\dot{\theta}_m\\ &+\omega_c L_a\frac{\omega_s B_m}{K_t}\int e_8 dt-\omega_c L_a\frac{\omega_s B_m}{K_t}\int\dot{\theta}_m dt\\ &-\omega_c L_a\frac{J_m\ddot{\theta}_m}{K_t}-\omega_c L_a\frac{\dot{\theta}_m B_m}{K_t}\\ &+\omega_c R_a\frac{\omega_s J_m}{K_t}\int e_8 dt-\omega_c R_a\frac{\omega_s J_m}{K_t}\int\dot{\theta}_m dt\\ &+\omega_c R_a\frac{\omega_s B_m}{K_t}\int\int e_8 dtdt\\ &-\omega_c R_a\frac{\omega_s B_m}{K_t}\int\int\dot{\theta}_m dtdt\\ &-\omega_c R_a\int[\frac{J_m\ddot{\theta}_m}{K_t}+\frac{\dot{\theta}_m B_m}{K_t}]dt\\ &+K_b\dot{\theta}_m. \end{aligned}\tag{48}$$

In (48), the mathematical terms $-\omega_c L_a\frac{\omega_s J_m}{K_t}\dot{\theta}_m$, $-\omega_c L_a\frac{\omega_s B_m}{K_t}\int\dot{\theta}_m dt$, $-\omega_c L_a\frac{J_m\ddot{\theta}_m}{K_t}$, $-\omega_c L_a\frac{\dot{\theta}_m B_m}{K_t}$, $K_b\dot{\theta}_m$, $-\omega_c R_a\frac{\omega_s J_m}{K_t}\int\dot{\theta}_m dt$, $-\omega_c R_a\frac{\omega_s B_m}{K_t}\int\int\dot{\theta}_m dtdt$ and $-\omega_c R_a\int[\frac{J_m\ddot{\theta}_m}{K_t}+\frac{\dot{\theta}_m B_m}{K_t}]dt$ can be seen as FFC. Thus, (48) can be regarded as a PII^2 controller with FFC. The proof of Lemma 5 is finished. ■

V. THE STABILITY ANALYSIS OF CLOSED-LOOP UNDER EQUIVALENCE CONTROL

In this part, the stability analysis of closed-loop for PI cascade, P cascade control and hybrid cascade control under equivalence control is presented.

As for two-stage PI cascade control, its transfer function can be described as:

$$\frac{X_{11}(s)}{X_{11}^{ref}(s)}=\frac{N1}{D1}.\tag{49}$$

where $X_{11}(s)$ and $X_{11}^{ref}(s)$ are Laplace transformation of $x_{11}(s)$ and $x_{11}^{ref}(s)$, respectively, $N1=a_{121}b_2kp_{11}ki_{21}s+a_{121}b_2ki_{11}ki_{21}+a_{121}b_2kp_{11}kp_{21}s^2+a_{12}b_2ki_{11}kp_{21}s$, $D1=s^4+kp_{21}b_2s^3+(ki_{21}b_2+a_{121}b_2kp_{11}kp_{21})s^2+a_{121}b_2kp_{11}ki_{21}s+a_{121}b_2ki_{11}kp_{21}s+a_{121}b_2ki_{11}ki_{21}$. The transfer function of its equivalence control is the same as equation (49). According to theory of frequency domain analysis, there exists $kp_{11}, ki_{11}, kp_{21}, ki_{21}$ such that the poles of the closed-loop transfer function (49) locate in the left half plane of the complex frequency domain.

As for three-stage PI cascade control, its transfer function can be depicted by

$$\frac{X_{11}(s)}{X_{11}^{ref}(s)}=\frac{N2}{D2}.\tag{50}$$

where $N2=(a_{121}a_{122}b_3kp_{11}kp_{21}kp_{31})s^3+q_1s^2+(a_{121}a_{122}b_3ki_{11}ki_{21}kp_{31}+a_{121}a_{122}b_3ki_{11}kp_{21}ki_{31}+a_{121}a_{122}b_3kp_{11}ki_{21}ki_{31})s+a_{121}a_{122}b_3ki_{11}ki_{21}ki_{31}$, and $q_1=a_{121}a_{122}b_3ki_{11}kp_{21}kp_{31}+a_{121}a_{122}b_3kp_{11}ki_{21}kp_{31}+a_{121}a_{122}b_3kp_{11}kp_{21}ki_{31}$, $D2=S^6+(kp_{31}b_3)s^5+(ki_{31}b_3+a_{122}b_3kp_{21}kp_{31})s^4+(a_{122}b_3ki_{21}kp_{31}+a_{122}b_3kp_{21}ki_{31}+a_{121}a_{122}b_3kp_{11}kp_{21}kp_{31})s^3+(a_{121}a_{122}b_3ki_{11}ki_{21}kp_{31}+a_{121}a_{122}b_3ki_{11}kp_{21}ki_{31}+a_{121}a_{122}b_3kp_{11}ki_{21}ki_{31})s+a_{121}a_{122}b_3ki_{11}ki_{21}ki_{31}+q_2s^2$.

$q_2=a_{121}a_{122}b_3ki_{11}kp_{21}kp_{31}+a_{121}a_{122}b_3kp_{11}ki_{21}kp_{31}+a_{121}a_{122}b_3kp_{11}kp_{21}ki_{31}+a_{122}b_3ki_{21}ki_{31}$. The transfer function of its equivalence control is the same as equation (50). According to theory of frequency domain analysis, there exists $kp_{11}, ki_{11}, kp_{21}, ki_{21}, kp_{31}, ki_{31}$ such that the poles of the closed-loop transfer function (50) locate in the left half plane of the complex frequency domain.

As for two-stage P cascade control, its transfer function can be presented as:

$$\frac{X_{11}(s)}{X_{11}^{ref}(s)}=\frac{N3}{D3}.\tag{51}$$

where $N3 = kp_{11}kp_{21}a_{121}b_2$, $D3 = s^2 + kp_{21}b_2s + kp_{11}kp_{21}a_{121}b_2$. The transfer function of its equivalence control is the same as equation (51). According to theory of frequency domain analysis, there exists kp_{11}, kp_{21} such that the poles of the closed-loop transfer function (51) locate in the left half plane of the complex frequency domain.

As for three-stage P cascade control, its transfer function can be illustrated as:

$$\frac{X_{11}(s)}{X_{11}^{ref}(s)} = \frac{N4}{D4}. \tag{52}$$

where $N4 = kp_{11}kp_{21}kp_{31}a_{121}a_{122}b_3$, $D4 = s^3 + kp_{31}b_3s^2 + kp_{31}kp_{21}a_{122}b_3s + kp_{11}kp_{21}kp_{31}a_{121}a_{122}b_3$. The transfer function of its equivalence control is the same as equation (52). According to theory of frequency domain analysis, there exists $kp_{11}, kp_{21}, kp_{31}$ such that the poles of the closed-loop transfer function (52) locate in the left half plane of the complex frequency domain.

As for the P-PI-PI cascade control, its transfer function can be shown as:

$$\frac{X_{11}(s)}{X_{11}^{ref}(s)} = \frac{N5}{D5}. \tag{53}$$

where $N5 = a_{121}a_{122}b_3kp_{11}kp_{21}kp_{31}s^2 + q_3s + a_{122}a_{121}b_3kp_{11}ki_{21}ki_{31}$, $q_3 = (a_{122}a_{121}b_3kp_{11}ki_{21}kp_{31} + a_{122}a_{121}b_3kp_{11}kp_{21}ki_{31})$, $D5 = s^5 + kp_{31}b_3s^4 + (ki_{31}b_3 + a_{122}b_3kp_{21}kp_{31})s^3 + (a_{122}b_3kp_{21}ki_{31} + a_{122}b_3ki_{21}kp_{31} + a_{122}a_{121}b_3kp_{11}kp_{21}kp_{31})s^2 + q_4s + a_{122}a_{121}b_3kp_{11}ki_{21}ki_{31}$ and $q_4 = (a_{122}b_3ki_{21}ki_{31} + a_{122}a_{121}b_3kp_{11}kp_{21}ki_{31} + a_{122}a_{121}b_3kp_{11}ki_{21}kp_{31})$. The transfer function of its equivalence control is the same as equation (53). According to theory of frequency domain analysis, there exists $kp_{11}, ki_{11}, ki_{21}, kp_{21}, kp_{31}$ such that the poles of the closed-loop transfer function (53) locate in the left half plane of the complex frequency domain.

As for the PI-P cascade control, its transfer function can be depicted as:

$$\frac{X_{11}(s)}{X_{11}^{ref}(s)} = \frac{N6}{D6}. \tag{54}$$

where $N6 = a_{121}b_2kp_{11}kp_{21}s + a_{121}b_2ki_{11}kp_{21}$, $D6 = s^3 + (b_2kp_{21})s^2 + (a_{121}b_2kp_{11}kp_{21})s + a_{121}b_2ki_{11}kp_{21}$. The transfer function of its equivalence control is the same as equation (54). According to theory of frequency domain analysis, there exists $kp_{11}, ki_{11}, kp_{21}$ such that the poles of the closed-loop transfer function (54) locate in the left half plane of the complex frequency domain.

VI. SIMULATION AND DISCUSSIONS

In order to verify the control effect of the proposed generalized PID control, some related simulation results are illustrated as follows: $R_a = 0.605\Omega$, $L_a = 0.210e^{-3}H$, $J_m = 86.57e^{-7}kg \cdot m^2$, $B_m = 4.2167e^{-5}Nm/(rad/s)$, $K_b = 0.0233V/(rad/s)$ and $K_t = 0.0234Nm/A$. The parameters of controllers are shown as follows: $\omega_c = 2000$, $\omega_s = 100$ and $k_p = 5$. We adopt integral time multiplied absolute error (ITAE), integral of squared error(ISE),integral of time multiplied squared error(ITSE) and integral of absolute error(IAE) to evaluate the performance of controllers.

A. PARAMETER TUNING RULES

In order to ensure the fairness of simulation comparison, we give the corresponding parameter tuning rules. The corresponding parameters of the PII^{2}D is from the equation (45). The corresponding parameters of the PII^{2}D with FFC is from the equation (45). The corresponding parameters of the PII^2 is from the equation (48). The corresponding parameters of the PII^2 with FFC is from the equation (48). The parameters of the above controllers can be calculated by using equation (45), equation (48), the parameters of (1) and (2), $\omega_c = 2000$, $\omega_s = 100$ and $k_p = 5$.

B. SIMULATION RESULTS AND DISCUSSIONS

For the constant speed tracking and constant position tracking conditions, the plant faces step disturbance (T_L step change) at t=5s.

1) CONSTANT SPEED TRACKING

Figure 15 illustrates that the closed-loop response of PII^{2}D control with FFC is the same as that of PI-PI control with FFC structure, which verifies that the PII^{2}D control with FFC is equivalence control of the PI-PI control with FFC structure. It also shows that the PII^2 control has slight overshoot without consideration of FFC. The worst one is the PI-PI control structure. From the ITAE value perspective, the PII^{2}D control with FFC and the PI-PI control with FFC are slightly better than the PII^{2}D control and PI-PI control structure in Figure 16.

However, from Figures 17-19, the PII^{2}D control is superior to the the PII^{2}D control with FFC and the PI-PI control with FFC in consideration of IAE, ISE and ITSE. Thus, the evaluation index of controller performance also affects the

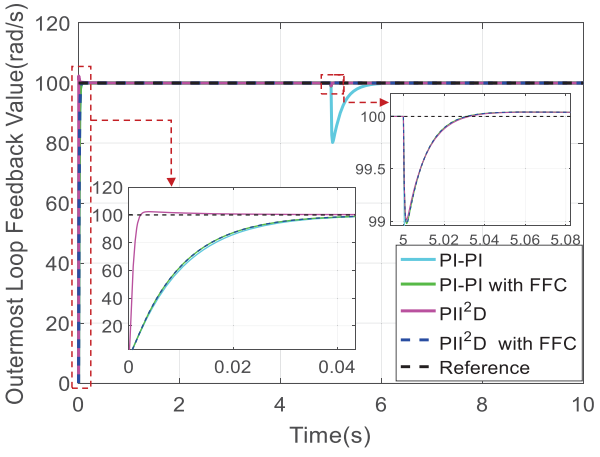

FIGURE 15. Comparison of PI-PI with FFC, PII^{2}D and PII^{2}D control with FFC for constant speed tracking.

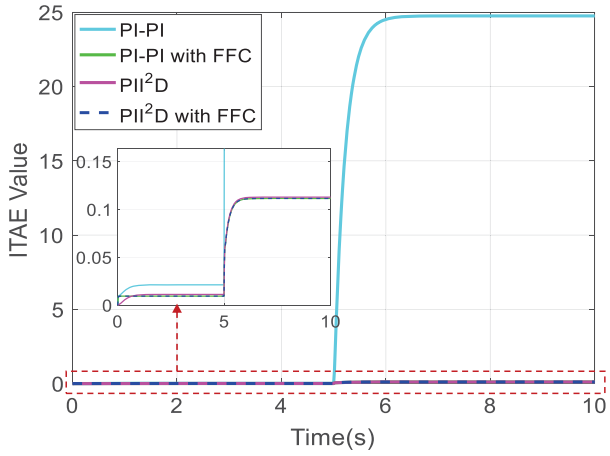

FIGURE 16. Comparison of PI-PI with FFC, PII^{2}D and PII^{2}D control with FFC for ITAE in constant speed tracking condition.

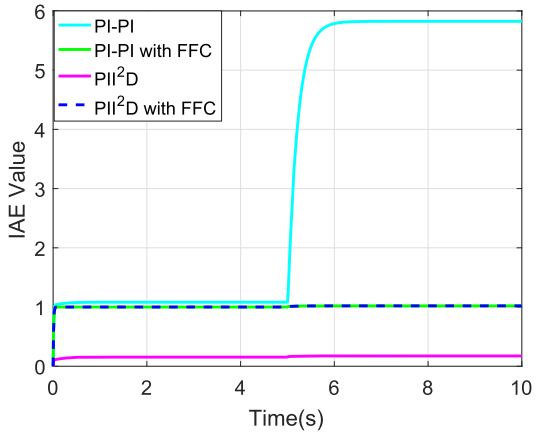

FIGURE 17. Comparison of PI-PI with FFC, PII^{2}D and PII^{2}D control with FFC for IAE in constant speed tracking condition.

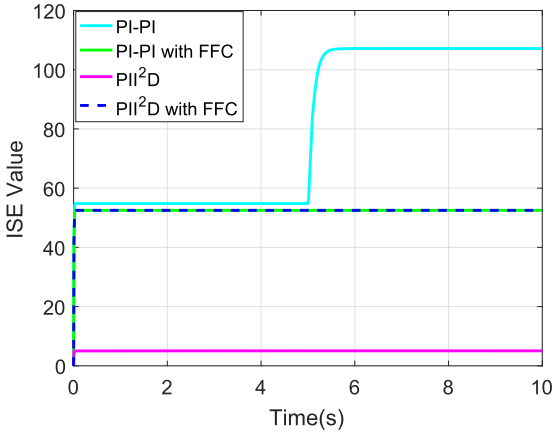

FIGURE 18. Comparison of PI-PI with FFC, PII^{2}D and PII^{2}D control with FFC for ISE in constant speed tracking condition.

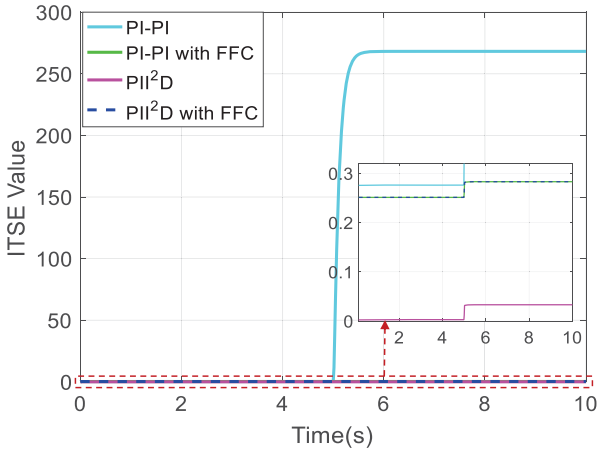

FIGURE 19. Comparison of PI-PI with FFC, PII^{2}D and PII^{2}D control with FFC for ITSE in constant speed tracking condition.

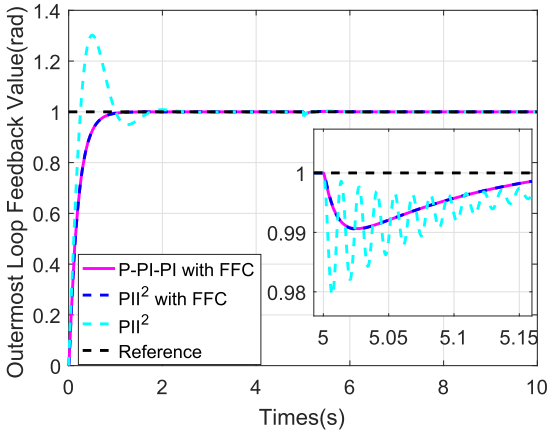

FIGURE 20. Comparison of P-PI-PI with FFC, PII^2 with FFC and PII^2 for position tracking.

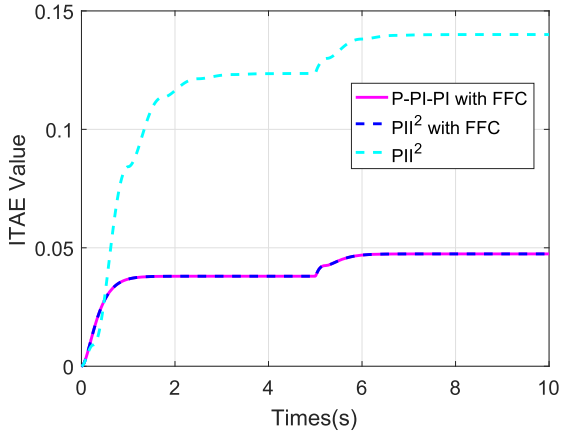

FIGURE 21. Comparison of P-PI-PI with FFC, PII^2 with FFC and PII^2 for ITAE in constant position tracking condition.

selection of controllers. Furthermore, other factors should be considered in the selection of controllers, which is beyond the scope of this article.

2) CONSTANT POSITION TRACKING

Furthermore, we can conclude that the FFC terms should be carefully considered from Figure 20 and Figure 21. Without the FFC terms, sinusoidal fluctuation exists when the plant

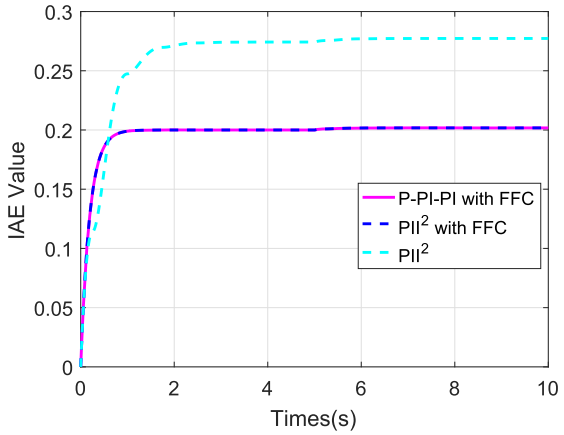

FIGURE 22. Comparison of P-PI-PI with FFC, PII^2 with FFC and PII^2 for IAE in constant position tracking condition.

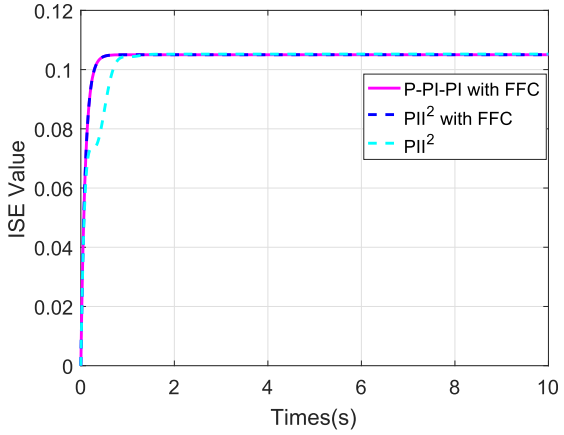

FIGURE 23. Comparison of P-PI-PI with FFC, PII^2 with FFC and PII^2 for ISE in constant position tracking condition.

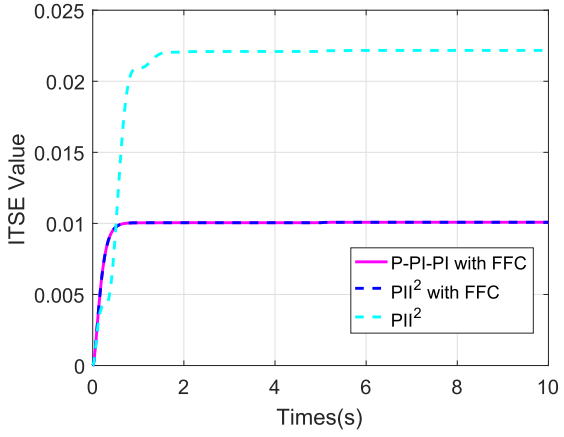

FIGURE 24. Comparison of P-PI-PI with FFC, PII^2 with FFC and PII^2 for ITSE in constant position tracking condition.

faces the disturbances, which is illustrated in Figure 20. Figures 20-24 validate that the PII^2 control with FFC is the equivalence control of the P-PI-PI with FFC. Figures 20-24 also illustrate that the PII^2 control is inferior to the P-PI-PI with FFC and PII^2 control with FFC.

VII. CONCLUSION

This paper has obtained the generalized PID control by equivalence analysis of cascade control for a class of cascade integral systems, which is based on the renewal type of the error. To be more specific, it has proved that the PI-PI cascade control, PI-PI-PI cascade control, P-PI-PI cascade control, PI-P cascade control, P-P cascade control and P-P-P cascade control can be interpreted as the proposed generalized PID control with FFC for ideal cascade integral systems. Moreover, the generalized PID control with FFC is extended to the non-ideal cascade integral systems, which has been verified in the MATLAB/Simulink environment. The possible future work will consider input delays based on the proposed analysis method.

ACKNOWLEDGMENT

The authors declare that they have no conflict of interest.

REFERENCES

[1] B. Sarlioglu and C. T. Morris, "More electric aircraft: Review, challenges, and opportunities for commercial transport aircraft," *IEEE Trans. Transport. Electrific.*, vol. 1, no. 1, pp. 54–64, Jun. 2015.

[2] W. Cao, B. C. Mecrow, G. J. Atkinson, J. W. Bennett, and D. J. Atkinson, "Overview of electric motor technologies used for more electric aircraft (MEA)," *IEEE Trans. Ind. Electron.*, vol. 59, no. 9, pp. 3523–3531, Sep. 2012.

[3] C. Guo, Q. Song, and W. Cai, "A neural network assisted cascade control system for air handling unit," *IEEE Trans. Ind. Electron.*, vol. 54, no. 1, pp. 620–628, Feb. 2007.

[4] Q.-C. Zhong and T. Hornik, "Cascaded current–voltage control to improve the power quality for a grid-connected inverter with a local load," *IEEE Trans. Ind. Electron.*, vol. 60, no. 4, pp. 1344–1355, Apr. 2013.

[5] W. Han, L. Xiong, and Z. Yu, "Interconnected pressure estimation and double closed-loop cascade control for an integrated electrohydraulic brake system," *IEEE/ASME Trans. Mechatronics*, vol. 25, no. 5, pp. 2460–2471, Oct. 2020, doi: 10.1109/TMECH.2020.2978534.

[6] S. Bozhko, T. Yang, and J. L. Peuvedic, "Development of aircraft electric starter–generator system based on active rectification technology," *IEEE Trans. Transport. Electrific.*, vol. 4, no. 4, pp. 985–996, Dec. 2018.

[7] J. Fu, J.-C. Maré, and Y. Fu, "Modelling and simulation of flight control electromechanical actuators with special focus on model architecting, multidisciplinary effects and power flows," *Chin. J. Aeronaut.*, vol. 30, no. 1, pp. 47–65, 2017.

[8] J. W. Bennett, B. C. Mecrow, A. G. Jack, and D. J. Atkinson, "A prototype electrical actuator for aircraft flaps," *IEEE Trans. Ind. Appl.*, vol. 46, no. 3, pp. 915–921, 2010.

[9] C. Liu, G. Luo, X. Duan, Z. Chen, Z. Zhang, and C. Qiu, "Adaptive LADRC-based disturbance rejection method for electromechanical servo system," *IEEE Trans. Ind. Appl.*, vol. 56, no. 1, pp. 876–889, Jan. 2020.

[10] R. M. Stephan, V. Hahn, J. Dastych, and H. Unbehauen, "Adaptive and robust cascade schemes for thyristor driven DC-motor speed control," *Automatica*, vol. 27, no. 3, pp. 449–461, May 1991.

[11] E. Panteley and R. Ortega, "Cascaded control of feedback interconnected nonlinear systems: Application to robots with AC drives," *Automatica*, vol. 33, no. 11, pp. 1935–1947, Nov. 1997.

[12] T. Kobaku, R. Jeyasenthil, S. Sahoo, and T. Dragicevic, "Experimental verification of robust PID controller under feedforward framework for a nonminimum phase DC–DC boost converter," *IEEE J. Emerg. Sel. Topics Power Electron.*, vol. 9, no. 3, pp. 3373–3383, Jun. 2021.

[13] X. Li, L. Guo, D. Huang, P. Li, L. Zhu, J. Zhu, Y. Wang, and C. Wang, "A reduced RLC impedance model for dynamic stability analysis of PI-controller-based DC voltage control of generic source-load two-terminal DC systems," *IEEE J. Emerg. Sel. Topics Power Electron.*, vol. 9, no. 6, pp. 7264–7277, Dec. 2021.

[14] A.-L. Alshalalfah, G. B. Hamad, and O. A. Mohamed, "Towards safe and robust closed-loop artificial pancreas using improved PID-based control strategies," *IEEE Trans. Circuits Syst. I, Reg. Papers*, vol. 68, no. 8, pp. 3147–3157, Aug. 2021.
[15] D. Zhai, L. An, J. Dong, and Q. Zhang, "Output feedback adaptive sensor failure compensation for a class of parametric strict feedback systems," *Automatica*, vol. 97, no. 11, pp. 48–57, Nov. 2018.
[16] J. Liu, S. Laghrouche, and M. Wack, "Observer-based higher order sliding mode control of power factor in three-phase AC/DC converter for hybrid electric vehicle applications," *Int. J. Control*, vol. 87, no. 6, pp. 1117–1130, Feb. 2014.
[17] H. An, J. Liu, C. Wang, and L. Wu, "Disturbance observer-based anti-windup control for air-breathing hypersonic vehicles," *IEEE Trans. Ind. Electron.*, vol. 63, no. 5, pp. 3038–3049, May 2016.
[18] D. Xu, J. Liu, X.-G. Yan, and W. Yan, "A novel adaptive neural network constrained control for a multi-area interconnected power system with hybrid energy storage," *IEEE Trans. Ind. Electron.*, vol. 65, no. 8, pp. 6625–6634, Aug. 2017.
[19] L. Wu, J. Liu, S. Vazquez, and S. K. Mazumder, "Sliding mode control in power converters and drives: A review," *IEEE/CAA J. Autom. Sinica*, vol. 9, no. 3, pp. 392–406, Mar. 2022.
[20] J. Liu, X. Shen, A. M. Alcaide, Y. Yin, J. I. Leon, S. Vazquez, L. Wu, and L. G. Franquelo, "Sliding mode control of grid-connected neutral-point-clamped converters via high-gain observer," *IEEE Trans. Ind. Electron.*, vol. 69, no. 4, pp. 4010–4021, Apr. 2022.
[21] X. Yu, T. Wang, and H. Gao, "Adaptive neural fault-tolerant control for a class of strict-feedback nonlinear systems with actuator and sensor faults," *Neurocomputing*, vol. 380, pp. 87–94, Mar. 2020.
[22] Q. Song and Y. D. Song, "Generalized PI control design for a class of unknown nonaffine systems with sensor and actuator faults," *Syst. Control Lett.*, vol. 64, pp. 86–95, Feb. 2014.
[23] S. Li and G. Tao, "Feedback based adaptive compensation of control system sensor uncertainties," *Automatica*, vol. 45, no. 2, pp. 393–404, 2009.
[24] C. Lin, Z. D. Wang, and F. W. Yang, "Observer-based networked control for continuous-time systems with random sensor delays," *Automatica*, vol. 45, no. 2, pp. 578–584, Feb. 2009.
[25] M. Liu, D. W. C. Ho, and P. Shi, "Adaptive fault-tolerant compensation control for Markovian jump systems with mismatched external disturbance," *Automatica*, vol. 58, pp. 5–14, Aug. 2015.
[26] L. An and G.-H. Yang, "Distributed optimal coordination for heterogeneous linear multiagent systems," *IEEE Trans. Autom. Control*, vol. 67, no. 12, pp. 6850–6857, Dec. 2022.

PING LIN received the Ph.D. degree in navigation guidance and control from the School of Control Science and Engineering, Dalian University of Technology, Dalian, China, in 2021.

He is currently working as a Postdoctoral Researcher with the Dalian University of Technology. His research interests include nonlinear systems, active disturbance rejection control, and generator control systems.

YAN SHI received the B.S. degree in automation and the Ph.D. degree in control theory and control engineering from Northeastern University, Shenyang, China, in 2013 and 2019, respectively.

He is currently a Research Associate with the Dalian University of Technology, Dalian, China. His research interests include switched systems, switched control, and aero-engine control systems.

XUE-FANG WANG (Member, IEEE) received the B.S. degree from the Ocean University of China, Qingdao College, in 2013, and the Ph.D. degree in control theory and control engineering from the Dalian University of Technology, Dalian, China, in 2019. From 2017 to 2019, she was a Visiting Scholar, working with Prof. Andrew R. Teel, at The University of California at Santa Barbara, Santa Barbara, CA, USA. She is currently a Research Associate with the Aeronautical and Automotive Engineering Department, Loughborough University. Her main research interests include multiagent systems, hybrid systems, distributed optimization problems, autonomous systems, and model predictive control.